Sparse Array Quiescent Beamformer Design Combining Adaptive and Deterministic Constraints

Xiangrong Wang, Moeness Amin (*IEEE Fellow*), Xianghua Wang, Xianbin Cao

***Abstract*—In this paper, we examine sparse array quiescent beamforming for multiple sources in interference-free environment. To maximize the output signal-to-noise ratio (SNR), the beamformer design comprises two intertwined stages, the determination of beamforming weights and the reconfiguration of array structure. The SNR maximization may produce high sidelobe levels, making the receiver vulnerable to interferences. We consider the problem of achieving maximum SNR beamforming subject to specified quiescent pattern constraints and, as such, combine both adaptive and deterministic approaches for sparse array configurations. We employ two convex relaxation methods and an iterative linear fractional programming algorithm to solve the non-convex antenna selection problem for sparse array beamformers. Simulation examples demonstrate that the array configuration plays a vital role in determining the beamforming performance in interference-free scenarios.**

***Index Terms*—Quiescent beamforming, Quadratic fractional, Frame approximation, Sequential convex programming**

I. Introduction

Antenna arrays are capable of performing beamforming, which makes them an effective tool for combating interference while providing certain gains towards desired sources [1]–[4]. The beamforming performance is not only dependent on the array weights but also on the array configuration [5]–[7]. For the same number of antennas, different array structures yield different maximum signal to noise ratios (SNRs) as well as different maximum signal to interference plus noise ratios (SINRs) [8], [9]. The opposite is also true, that is, for the same array configuration, beamformers can assume different characteristics and performances. As such, sparse array design should utilize both the array structure and array weights towards achieving the optimum performance. Beamforming can be broadly classified into deterministic and adaptive [10]. The former focuses on synthesizing beampatterns with prescribed mainlobe width and reduced sidelobe levels [11], [12]. Adaptive beamforming, on the other hand, is influenced by the environment and incorporates, in addition to noise characteristics, the source and interference signals or data statistics which are present in the array field of view (FOV). Different from the determinitic array design, pattern nulls of adaptive beamformers are formed in the direction of existing interferences to eliminate, or significantly reduce, the interference power at the output of the array [13].

In this paper, we consider the general case of optimum beamformer design when dealing with multiple desired sources. That is, the dimension of the desired signal subspace, in an interference-free environment, is arbitrary and not necessarily confined to a unit value. This case is encountered with multiple communication emitters in the FOV, and also occurs in radar tracking of multiple targets. If maximum SNR is the array design objective, then the optimum array weight vector for multiple source signals impinging on the receiver, is the principal eigenvector of the source covariance matrix [10]. Clearly, the optimum beamformrer does not guarantee equal sensitivities towards all sources, which may not be desired, especially when the sources are identically weak and equally important. Thus, it becomes necessary to examine the design of optimum adaptive beamformer that maximizes the output SNR while providing approximately equal responses towards all sources. There are other types of beamformers proposed in the literature to incorporate unused degrees of freedom (DoF) into the beamformer quiescent response for a uniform linear array or a given array structure [14], [15]. However, no consideration has been given to the problem of optimum sparse array configuration and antenna selections dealing with multiple desired sources in interference-free environment, and applying quiescent pattern constraints.

The problem of adaptive beamformer design, incorporating both the array configuration and the array weights, without sidelobe constraints was examined in our recent work [16]. Although superior to deterministic design, high sidelobe levels may constitute a potential problem in adaptive beamformer, specially, when directional interferers are suddenly switched on. This mandates the selection of antenna positions according to a set of desirable constraints on the beamformer sidelobes [14]. As such, it is important to seek a sparse array configuration that maximizes the output SNR with well-controlled sidelobes, which constitutes the main novelty of this paper. We consider two beamformers with controlled sidelobe levels for maximizing the output SNR. The first is fully adaptive and provides the maximum SNR (the MSNR beamformer) without concerning with homogeneity of array responses towards different sources. The second beamformer is semi-adaptive and strives to reach desired response values while utilizing the source spatial correlations adaptively to minimize output SNR degradation. Two convex relaxation approaches and an iterative linear fractional programming

Xiangrong Wang and Xianbin Cao are with School of Electronic and Information Engineering, Beihang University, Beijing, China, 100191. The work of Dr. Wang and Dr. Cao is supported by National Key Research Development Program under Grant No. 2016YFB1200100 and National Natural Science Foundation of China under Grant No. 61701016. Moeness Amin is with Center for Advanced Communications, Villanova University, PA, USA, 19085. The work of Dr. Amin is supported by the National Science Foundation under Grant No. AST-1547420. Xianghua Wang (corresponding author) is with College of Electrical Engineering and Automation, Shandong University of Science and Technology, Qingdao, China, 266590. E-mail: xrwang@buaa.edu.cn, moeness.amin@villanova.edu, xianghuaw@pku.edu.cn. Part of the work is presented at ICASSP 2017.

(ILFP) algorithm are proposed to solve underlying sparse array beamformer problems.

Although the deterministic beamformer design has been extensively investigated in the literature [17]–[20], it focuses on thinned arrays and synthesizes either focused or shaped beampatterns. The former targets the single-source scenario, whereas the latter responds to a spatially distributed source. However, neither approach has addressed the case of multiple discrete sources. Moreover, since the lower-bound constraints on the mainlobe region are non-convex, the assumption of conjugate symmetric beamforming weights is typically imposed on the shaped-beampattern synthesis [17]. This assumption halves the available DoFs. One method for circumventing the loss of DoFs is the utilization of semi-definite programming, however the relaxation of rank-one constraint cannot guarantee a unique and reliable solution [18]. The state-of-the-art array thinning techniques employ sparsity-promoting functions, such as l_1-norm [21]–[23] and Bayesian inference [24], causing the number of selected antennas to be uncontrollable and completely determined by the applied algorithms. In this paper, we reformulate the deterministic beamformer design problem such that the number of antennas is predefined and the symmetric assumption is eliminated. This constitutes the second main contribution of this paper.

A brief description of the notations used in this paper is provided as follows. The symbols $\mathbb{N}$ and $\mathbb{C}$ denote the sets of integer and complex numbers respectively. The operation $\text{diag}(\mathbf{x})$ means a diagonal matrix with the vector $\mathbf{x}$ populating along its diagonal. We use x_i to denote the ith entry of the vector $\mathbf{x}$, while the bold $\mathbf{x}_i$ is the vector indexed by i. The index set with cardinality K is denoted by $\mathcal{J}_K$. $\mathbf{x}(\mathcal{J})$ and $\mathbf{X}(\mathcal{J})$ remain the entries (columns) indexed by $\mathcal{J}$ while deletes others. We simplify "subject to" with the abbreviation "s.t.".

The rest of this paper is organized as follows: We formulate the problem in section II. We introduce the adaptive beamformer design without quiescent pattern constraints in section III. The deterministic beamformer design is reformulated in section IV. Formulation of sparse array MSNR and semi-adaptive beamformer design with sidelobe constraints is elucidated in section V. Simulation results, presented in section VI, validate the effectiveness of proposed design methods. Finally, concluding remarks are provided in section VII.

II. Problem Formulation

Consider a linear array of N isotropic antennas with positions specified by multiple integer of unit inter-element spacing $x_n d, x_n \in \mathbb{N}, n = 1, \ldots, N$. Note that the linear array configuration is adopted for simplicity, and all proposed algorithms in this paper are applicable to two dimensional arrays. Suppose that p source signals are impinging on the array from directions $\{\theta_1, \ldots, \theta_p\}$ with spatial steering vectors specified by,

$$\mathbf{u}_k = [e^{jk_0 x_1 d\cos\theta_k}, \cdots, e^{jk_0 x_N d\cos\theta_k}]^T, k = 1, \ldots, p. \quad (1)$$

The wavenumber is defined as $k_0 = 2\pi/\lambda$ with λ being the wavelength and ^{T} denotes transpose operation. The received signal at time instant t is given by,

$$\mathbf{x}(t) = \mathbf{U}\mathbf{s}(t) + \mathbf{n}(t), \quad (2)$$

where $\mathbf{U} = [\mathbf{u}_1, \ldots, \mathbf{u}_p] \in \mathbb{C}^{N\times p}$ is the source array manifold matrix. In the above equation, $\mathbf{s}(t) \in \mathbb{C}^p$ denotes the source vector at time instant t and $\mathbf{n}(t) \in \mathbb{C}^N$ the received noise vector. The output of the N-antenna beamformer is given by,

$$y(t) = \mathbf{w}^H\mathbf{x}(t), \quad (3)$$

where $\mathbf{w} \in \mathbb{C}^N$ is the complex vector of beamformer weights and ^{H} stands for Hermitian operation. With additive Gaussian noise, i.e., $\mathbf{n}(t) \sim \mathcal{CN}(\mathbf{0}, \sigma_n^2\mathbf{I})$, where σ_n^2 denotes the noise power level, and in the absence of interfering sources, the optimal weight vector for maximizing the output SNR is given by [10],

$$\mathbf{w} = \mathcal{P}\{\mathbf{R}_s\} = \mathcal{P}\{\mathbf{U}\mathbf{C}_s\mathbf{U}^H\}. \quad (4)$$

where $\mathcal{P}\{\cdot\}$ denotes the principal eigenvector of the matrix, $\mathbf{R}_s$ is defined as $\mathbf{R}_s = \mathbf{U}\mathbf{C}_s\mathbf{U}^H$ with $\mathbf{C}_s = E\{\mathbf{s}(t)\mathbf{s}^H(t)\}$ being the source auto-correlation matrix. The output SNR is,

$$\text{SNR} = \frac{\mathbf{w}^H\mathbf{R}_s\mathbf{w}}{\mathbf{w}^H\mathbf{R}_n\mathbf{w}} = \frac{\lambda_{\max}\{\mathbf{R}_s\}}{\sigma_n^2} = \frac{\|\mathbf{R}_s\|_2}{\sigma_n^2}. \quad (5)$$

Clearly, array configuration affects the output SNR of the MSNR beamformer through the term of $\|\mathbf{R}_s\|_2$. Note that the optimal weight vector in Eq. (4) is a linear combination of the source steering vectors.

Intuitively, the MSNR beamformer favours the strong and closely-spaced sources for maximizing the output SNR. Therefore, one disadvantage of the MSNR beamformer is that it cannot guarantee equal sensitivities towards all sources, which may not be desirable in practice, specifically when all sources should be equally served by the receiver. Although the deterministic beamformer with predefined mainlobes and controlled sidelobe level can provide exact and equal sensitivities, it does not strive to maximize the output SNR. To illustrate, suppose the array response towards the p desired sources is determined by the vector $\mathbf{r} \in \mathbb{C}^p$, i.e.,

$$\mathbf{U}^H\mathbf{w} = \mathbf{r} \text{ and } \mathbf{w}^H\mathbf{w} = 1. \quad (6)$$

Then, the output SNR of the deterministic beamformer can be calculated as,

$$\text{SNR} = \frac{\mathbf{w}^H\mathbf{R}_s\mathbf{w}}{\mathbf{w}^H\mathbf{R}_n\mathbf{w}} = \frac{\mathbf{r}^H\mathbf{C}_s\mathbf{r}}{\sigma_n^2}, \quad (7)$$

which is a fixed value, independent of the array configuration.

In order to define a role for SNR in deterministic sparse array beamformer design, and strike a compromise between preset beamformer characteristics and SNR performance, we first relax the condition of exact array response and attempt to only offer approximate equal gains towards all sources of interest. This is achieved by first expressing the weight vector as a function of sources steering vectors, i.e.,

$$\mathbf{w} = \sum_{k=1}^{p} \beta_k\mathbf{u}_k, \quad (8)$$

with specified coefficients $\beta_k, k = 1, \ldots, p$. Accordingly, the array response towards the ith source is given by,

$$r_i = \mathbf{u}_i^H\mathbf{w} = N\beta_i + \sum_{k=1, k\neq i}^{p} \beta_k\rho_{ik}, \quad (9)$$

where $\rho_{ik} = \mathbf{u}_i^H \mathbf{u}_k$ denotes the spatial correlation between the ith and kth sources. Notably, the array response cannot be exactly described by the coefficient vector $\beta = [\beta_1, \ldots, \beta_p]^T$ due to the non-zero correlations, and as such, the case of equal coefficients will not necessarily lead to equal gain, unless the sources are spatially orthogonal. Using Eq. (8), the output SNR of the beamformer becomes,

$$\text{SNR} = \frac{\mathbf{w}^H \mathbf{R}_s \mathbf{w}}{\mathbf{w}^H \mathbf{R}_n \mathbf{w}} = \frac{\beta^H \mathbf{U}^H \mathbf{U} \mathbf{C}_s \mathbf{U}^H \mathbf{U} \beta}{\sigma_n^2 \beta^H \mathbf{U}^H \mathbf{U} \beta}, \tag{10}$$

which is influenced by the array configuration through the spatial correlations among sources in the matrix $\mathbf{U}^H\mathbf{U} = [\rho_{ik}, i, k = 1, \ldots, p]$. In essence, spatial correlations cause the array response to deviate from the specified coefficient vector β and, thus, leverage the array configuration to further improve output SNR compared to deterministic beamformers.

III. Sparse Array MSNR Beamformer Design Without Sidelobe Constraints

Given the number of antennas and a specific beamformer, array configurations remain a source of flexibility and can allocate DoFs, i.e. antenna positions, towards achieving the optimum design of maximizing the output SNR of quiescent beamformers. Suppose that there are N grid points out of which K antennas can be placed. Denote an antenna selection vector $\mathbf{z} = [z_i, i = 1, \ldots, N] \in \{0, 1\}^N$ with "zero" entry for a discarded antenna and "one" entry for a selected antenna. As steering vectors are directional, the steering vector of the selected sparse array can be expressed as $\mathbf{z} \odot \mathbf{u}_k, k = 1, \ldots, p$, with $\odot$ denoting element-wise product. In addition, we define a selection matrix as $\mathbf{Z} = \{0, 1\}^{K \times N}$ for a simple mathematical derivation in the sequel, with a "one" entry in the ith row and the jth column, where $i = 1, \ldots, K$ and $z_j = 1, j \in \{1, \ldots, N\}$. Thus, the selection vector $\mathbf{z}$ and the selection matrix $\mathbf{Z}$ are inner-connected and their relationship can be expressed as $\mathbf{Z}\mathbf{Z}^T = \mathbf{I}$ and $\mathbf{Z}^T\mathbf{Z} = \text{diag}(\mathbf{z})$. The implementation of antenna selection can also be expressed in terms of the selection matrix $\mathbf{Z}$ as $\mathbf{u}_k \odot \mathbf{z} = \mathbf{Z}\mathbf{u}_k, k = 1, \ldots, p$ and, accordingly, $\mathbf{U}(\mathbf{z}) = [\mathbf{u}_k \odot \mathbf{z}, k = 1, \ldots, p] = \mathbf{Z}\mathbf{U}$. Ideally and from Eq. (5), the optimum sparse array MSNR beamformer should be reconfigured through antenna selection such that the spectral norm of reduced-dimensional source covariance matrix $\|\mathbf{R}_s(\mathbf{z})\|_2$ is maximized. That is,

$$\begin{aligned} \max_{\mathbf{z}} \quad & \left\{ \|\mathbf{R}_s(\mathbf{z})\|_2 = \|\mathbf{U}(\mathbf{z}) \mathbf{C}_s \mathbf{U}^H(\mathbf{z})\|_2 \right\}, \\ \text{s.t.} \quad & \mathbf{z} \in \{0, 1\}^N, \ \mathbf{1}^T \mathbf{z} = K, \end{aligned} \tag{11}$$

where $\mathbf{1}$ is a column vector of all ones.

The method of implementing eigenvalue decomposition for each subset of K sensor locations is computationally prohibitive, even with a small number of sensors. Towards solving Eq. (11), we first relax the binary constraints $\mathbf{z} \in \{0, 1\}^N$ to a box constraint $0 \leq \mathbf{z} \leq 1$, as the spectral norm of a matrix is convex and the global maximizer of a convex function locates at the extreme points of the polyhedron $0 \leq \mathbf{z} \leq 1, \mathbf{1}^T\mathbf{z} = K$ [25]. This satisfies the boolean property of the selection variable automatically and eliminates the binary constraints in the problem formulation. Furthermore, maximizing a convex function directly as per Eq. (11) is a non-convex optimization problem, thus we resort to the following two methods for convex relaxation.

A. Iterative Affine Approximation

Define the column vectors of $\mathbf{U}^H$ as $\bar{\mathbf{u}}_i, i = 1, \ldots, N$, and $\tilde{\mathbf{u}}_i = \mathbf{C}_s^{1/2} \bar{\mathbf{u}}_i$. According to the definition of matrix spectral norm [26], the objective function in Eq. (11) is equivalent to,

$$\begin{aligned} f(\mathbf{z}) &= \| \sum_{i=1}^N z_i \tilde{\mathbf{u}}_i \tilde{\mathbf{u}}_i^H \|_2, \\ &= \max_{\|\mathbf{b}\|_2 = 1} \sum_{i=1}^N z_i \mathbf{b}^H \tilde{\mathbf{u}}_i \tilde{\mathbf{u}}_i^H \mathbf{b}, \\ &= \sum_{i=1}^N z_i \tilde{\mathbf{b}}^H \tilde{\mathbf{u}}_i \tilde{\mathbf{u}}_i^H \tilde{\mathbf{b}}, \end{aligned} \tag{12}$$

where $\tilde{\mathbf{b}}$ is clearly the principal eigenvector of the matrix $\sum_{i=1}^N z_i \tilde{\mathbf{u}}_i \tilde{\mathbf{u}}_i^H$. Since the convex objective function can be approximated iteratively by its affine global under-estimator, $f(\mathbf{z})$ in the $(k+1)$th iteration can be approximated based on the previous solution $\mathbf{z}^{(k)}$ by,

$$f(\mathbf{z}) \approx f(\mathbf{z}^{(k)}) + g(\mathbf{z}^{(k)})^T (\mathbf{z} - \mathbf{z}^{(k)}), \tag{13}$$

where $g(\mathbf{z}^{(k)})$ is the gradient of $f(\mathbf{z})$ evaluated at the point $\mathbf{z}^{(k)}$. The ith entry of $g(\mathbf{z}^{(k)})$ is obtained from Eq. (12),

$$g(z_i^{(k)}) = \frac{\partial f}{\partial z_i} \mid_{\mathbf{z}^{(k)}} = \tilde{\mathbf{b}}^{(k)H} \tilde{\mathbf{u}}_i \tilde{\mathbf{u}}_i^H \tilde{\mathbf{b}}^{(k)}. \tag{14}$$

Here, $\tilde{\mathbf{b}}^{(k)}$ denotes the principal eigenvector of the matrix $\sum_{i=1}^N z_i^{(k)} \tilde{\mathbf{u}}_i \tilde{\mathbf{u}}_i^H$. Thus, the non-convex selection problem can be relaxed iteratively as,

$$\begin{aligned} \max_{\mathbf{z}} \quad & f(\mathbf{z}^{(k)}) + g(\mathbf{z}^{(k)})^T (\mathbf{z} - \mathbf{z}^{(k)}), \\ \text{s.t.} \quad & 0 \leq \mathbf{z} \leq 1, \ \mathbf{1}^T \mathbf{z} = K. \end{aligned} \tag{15}$$

This transforms the non-convex MSNR beamformer design in Eq. (11) into a linear programming (LP) problem as Eq. (15), and, in turn, significantly alleviates the computational complexity. The iterative approximations are referred to as sequential convex progamming (SCP) [27]. Note that SCP is a local heuristic and its performance depends on the initial point $\mathbf{z}^{(0)}$. It is, therefore, typical to initialize the algorithm with several feasible points $\mathbf{z}^{(0)}$ and the final choice is the one with the maximum objective value over the different runs.

B. Frame Based Approximation

Frames are signal representation tools that are redundant, which means that the number of frames is more than the dimension of the denoted signal space, and thus no longer linearly independent as bases. They are often used when there is a need for more flexibility in choosing a representation [28]. A family $\hat{\mathbf{E}} = \{\hat{\mathbf{e}}_i\}_{i \in \mathcal{I}}$ with the index set $\mathcal{I}$ in a Hilbert space $\mathcal{H}$ is called a frame, if there exists two constants $0 < \alpha \leq \beta < \infty$, such that for all vectors $\mathbf{h}$ in $\mathcal{H}$, we have

$$a\|\mathbf{h}\|^2 \leq \sum_{i \in \mathcal{I}} |\langle \hat{\mathbf{e}}_i, \mathbf{h} \rangle|^2 \leq b\|\mathbf{h}\|^2, \tag{16}$$

where $\langle \hat{\mathbf{e}}_i, \mathbf{h} \rangle = \hat{\mathbf{e}}_i^H \mathbf{h}$ and a, b are named frame bounds. Tight frames (TFs) are frames with equal frame bounds, that is, $a = b$. Parseval TFs (PTFs) are TFs with frame bound $a = b = 1$. Denote the frame operator as $\mathbf{\Phi} = \hat{\mathbf{E}}\hat{\mathbf{E}}^H$, then the definition of frame implies that,

$$a\mathbf{I} \leq \mathbf{\Phi} \leq b\mathbf{I}. \tag{17}$$

Accordingly, the frame operator $\mathbf{\Phi} = \hat{\mathbf{E}}\hat{\mathbf{E}}^H = \mathbf{I}$ for PTF. Note that the Grammian $\mathbf{G} = \hat{\mathbf{E}}^H\hat{\mathbf{E}} \neq \mathbf{I}$.

Naimark Theorem: ([29], [30]) A set $\hat{\mathbf{E}} = \{\hat{\mathbf{e}}_i\}_{i\in\mathcal{I}}$ in a Hilbert space $\mathcal{H}$ is a PTF for $\mathcal{H}$ if and only if there is a larger Hilbert space $\mathcal{K}$, $\mathcal{H} \subset \mathcal{K}$, and a set of orthonormal bases $\{\mathbf{e}_i\}_{i\in\mathcal{I}}$ for $\mathcal{K}$ so that the orthogonal projection $\mathbf{P}$ of $\mathcal{K}$ onto $\mathcal{H}$ satisfies: $\mathbf{P}\mathbf{e}_i = \hat{\mathbf{e}}_i$, for all $i \in \mathcal{I}$.

The Naimark Theorem implies every PTF can be obtained by projecting a set of orthonormal bases from a larger space to a lower space. This process is called seeding. Recalling the definition of the selection matrix $\mathbf{Z}$, the columns of $\mathbf{Z}$ are obtained by projecting the N-dimensional identity matrix $\mathbf{I}$ to the K-dimensional lower space, and they constitute a PTF. Assume that the source auto-correlation matrix $\mathbf{C}_s$ is known a priori or previously estimated. Then, the principal eigenvector of the source covariance matrix associated with the array of fully populated grid of N sensors can be provided through eigenvalue decomposition of $\mathbf{R}_s$, i.e.,

$$\mathbf{R}_s = \mathbf{U}\mathbf{C}_s\mathbf{U}^H = \mathbf{E}\mathbf{\Lambda}\mathbf{E}^H, \tag{18}$$

where $\mathbf{\Lambda} = \text{diag}(\lambda_1, \ldots, \lambda_p, 0, \ldots, 0)$ with the p eigenvalues along its diagonal in a descending order and $\mathbf{e}_i, i = 1, \ldots, N$ are corresponding eigenvectors. According to the Naimark Theorem, a PTF can be obtained by seeding from a set of eigenbasis $\mathbf{E}$ by deleting a subset of rows of $\mathbf{E}$. We denote the result as,

$$\hat{\mathbf{E}} = [\hat{\mathbf{e}}_1, \ldots, \hat{\mathbf{e}}_N] = [\mathbf{E}^T(\mathcal{J})]^T, \tag{19}$$

where $\mathcal{J} \subset \{1, \ldots, N\}$ is the index set of remained columns of the matrix $\mathbf{E}^T$. Clearly, $\|\hat{\mathbf{e}}_i\|_2 \neq 1, i = 1, \ldots, N$, and thus $\mathbf{G} = \hat{\mathbf{E}}^H\hat{\mathbf{E}} \neq \mathbf{I}$. However, we still have $\mathbf{\Phi} = \hat{\mathbf{E}}\hat{\mathbf{E}}^H = \mathbf{I}$. Therefore, the column vectors of $\hat{\mathbf{E}}$ constitute a PTF and the source covariance matrix after antenna selection can be represented in terms of the PTF as,

$$\hat{\mathbf{R}}_s = \mathbf{Z}\mathbf{U}\mathbf{C}_s\mathbf{U}^H\mathbf{Z}^T = (\mathbf{Z}\mathbf{E})\mathbf{\Lambda}(\mathbf{Z}\mathbf{E})^H = \hat{\mathbf{E}}\mathbf{\Lambda}\hat{\mathbf{E}}^H. \tag{20}$$

Furthermore, the frame $\hat{\mathbf{e}}_1 = \mathbf{Z}\mathbf{e}_1$ still possesses the largest coefficient λ_1. For this reason and based on the PFT argument, we consider $\hat{\mathbf{e}}_1/\|\hat{\mathbf{e}}_1\|_2$ to closely mimic the principal eigenvector of the selected sparse array. Accordingly, the optimum weight vector for maximizing output SNR of the sparse array can be approximated by $\mathbf{w} \approx \hat{\mathbf{e}}_1/\|\hat{\mathbf{e}}_1\|_2$. Combining this result with the definition of the spectral norm of the source covariance matrix, we obtain the lower bound, i.e.,

$$\begin{aligned} \|\mathbf{U}(\mathbf{z})\mathbf{C}_s\mathbf{U}^H(\mathbf{z})\|_2 &= \max_{\|\mathbf{b}\|_2=1} \mathbf{b}^H\mathbf{U}(\mathbf{z})\mathbf{C}_s\mathbf{U}^H(\mathbf{z})\mathbf{b}, \\ &\geq \frac{\hat{\mathbf{e}}_1^H\mathbf{U}(\mathbf{z})\mathbf{C}_s\mathbf{U}^H(\mathbf{z})\hat{\mathbf{e}}_1}{\|\hat{\mathbf{e}}_1\|_2^2}, \\ &= \frac{\mathbf{e}_1^H\text{diag}(\mathbf{z})\mathbf{U}\mathbf{C}_s\mathbf{U}^H\text{diag}(\mathbf{z})\mathbf{e}_1}{\mathbf{e}_1^H\text{diag}(\mathbf{z})\mathbf{e}_1}. \end{aligned} \tag{21}$$

Therefore, the sparse array MSNR beamformer design can be formulated as,

$$\begin{aligned} \max_{\mathbf{z}} \quad & \frac{\mathbf{e}_1^H\text{diag}(\mathbf{z})\mathbf{U}\mathbf{C}_s\mathbf{U}^H\text{diag}(\mathbf{z})\mathbf{e}_1}{\mathbf{e}_1^H\text{diag}(\mathbf{z})\mathbf{e}_1}, \\ \text{s.t.} \quad & \mathbf{z} \in \{0,1\}^N,\ \mathbf{1}^T\mathbf{z} = K. \end{aligned} \tag{22}$$

The objective function in Eq. (22) can be manipulated into a quasi-convex quadratic fractional problem [27], solved by the algorithm proposed in section V.

IV. Deterministic Beamformer Design

We still consider the p discrete desired sources. Denote the sidelobe region as Ω, and sample Ω with a set of predefined discrete angles $\{\theta_{s1}, \ldots, \theta_{sL}\}$. Their respective steering vectors of the fully populated array are denoted as $\mathbf{a}_i, i = 1, \ldots, L$ and the corresponding steering matrix is $\mathbf{A} = [\mathbf{a}_1, \ldots, \mathbf{a}_L]$. The controlled sidelobes can be formulated as $|\mathbf{w}^H\mathbf{A}| \leq \epsilon$, where ϵ denotes the desired sidelobe level. Clearly, the sample number L should be sufficiently large for a better-shaped quiescent pattern, which inevitably increases the number of constraints and reducing the DoF to shape the pattern over other angular regions. Based on the frame theory explained in section III-B, we implement eigenvalue decomposition $\mathbf{A}\mathbf{A}^H = \mathbf{V}\mathbf{\Gamma}\mathbf{V}^H$ and utilize the set of dominant frames $\mathbf{V}(\mathcal{J}) = \{\mathbf{v}_i, i \in \mathcal{J}\}$ to represent sidelobe region. The sidelobe constraints can then be expressed as $\mathbf{V}^H(\mathcal{J})\mathbf{w} = 0$ [10]. The deterministic array design with exactly K selected antennas is formulated as,

$$\begin{aligned} \text{Find} \quad & \mathbf{w}, \\ \text{s.t.} \quad & \mathbf{w}^H\mathbf{u}_i\mathbf{u}_i^H\mathbf{w} \leq 1 + \delta, i = 1, \ldots, p, \\ & \mathbf{w}^H\mathbf{u}_i\mathbf{u}_i^H\mathbf{w} \geq 1 - \delta, i = 1, \ldots, p, \\ & \mathbf{V}^H(\mathcal{J})\mathbf{w} = 0, \\ & \text{or } \mathbf{w}^H\mathbf{a}_i\mathbf{a}_i^H\mathbf{w} \leq \epsilon, i = 1, \ldots, L, \\ & \|\mathbf{w}\|_0 = K. \end{aligned} \tag{23}$$

where δ represents the acceptable mainlobe ripple. Different from the adaptive beamformer design with a binary selection variable $\mathbf{z}$, the variable $\mathbf{w}$ in the deterministic design in Eq. (23) is only required to be sparse with cardinality K. We split the $N \times 1$ weight variable into real and imaginary parts and stack them as a $2N \times 1$ vector, i.e., $\tilde{\mathbf{w}} = [\mathbb{R}(\mathbf{w})^T, \mathbb{I}(\mathbf{w})^T]^T$. Then, the problem of deterministic array design can be transformed from the complex domain to the real domain, i.e.,

$$\begin{aligned} \text{Find} \quad & \tilde{\mathbf{w}}, && \text{(24a)} \\ \text{s.t.} \quad & \tilde{\mathbf{w}}^H\tilde{\mathbf{U}}_i\tilde{\mathbf{w}} \leq 1 + \delta, i = 1, \ldots, p, && \text{(24b)} \\ & \tilde{\mathbf{w}}^H\tilde{\mathbf{U}}_i\tilde{\mathbf{w}} \geq 1 - \delta, i = 1, \ldots, p, && \text{(24c)} \\ & \tilde{\mathbf{V}}^H(\mathcal{J})\tilde{\mathbf{w}} = 0, && \text{(24d)} \\ & \text{or } \tilde{\mathbf{w}}^H\tilde{\mathbf{A}}_i\tilde{\mathbf{w}} \leq \epsilon, i = 1, \ldots, L && \text{(24e)} \\ & \|\mathbf{P}_u(\tilde{\mathbf{w}} \odot \tilde{\mathbf{w}}) + \mathbf{P}_l(\tilde{\mathbf{w}} \odot \tilde{\mathbf{w}})\|_0 = K. && \text{(24f)} \end{aligned}$$

where the matrices $\tilde{\mathbf{U}}_i$, $\tilde{\mathbf{A}}_i$ and $\tilde{\mathbf{V}}(\mathcal{J})$ are defined as,

$$\tilde{\mathbf{U}}_i = \begin{bmatrix} \mathbb{R}(\mathbf{u}_i\mathbf{u}_i^H) & -\mathbb{I}(\mathbf{u}_i\mathbf{u}_i^H) \\ \mathbb{I}(\mathbf{u}_i\mathbf{u}_i^H) & \mathbb{R}(\mathbf{u}_i\mathbf{u}_i^H) \end{bmatrix},\ i = 1, \ldots, p \tag{25}$$

$$\tilde{\mathbf{A}}_i = \begin{bmatrix} \mathbb{R}(\mathbf{a}_i\mathbf{a}_i^H) & -\mathbb{I}(\mathbf{a}_i\mathbf{a}_i^H) \\ \mathbb{I}(\mathbf{a}_i\mathbf{a}_i^H) & \mathbb{R}(\mathbf{a}_i\mathbf{a}_i^H) \end{bmatrix},\ i = 1, \ldots, L \tag{26}$$

and

$$\tilde{\mathbf{V}}(\mathcal{J}) = \begin{bmatrix} \mathbb{R}(\mathbf{V}(\mathcal{J})) & -\mathbb{I}(\mathbf{V}(\mathcal{J})) \\ \mathbb{I}(\mathbf{V}(\mathcal{J})) & \mathbb{R}(\mathbf{V}(\mathcal{J})) \end{bmatrix}, \tag{27}$$

respectively. The selection matrices $\mathbf{P}_u = [\mathbf{I}_{N\times N}, \mathbf{0}_{N\times N}]$ and $\mathbf{P}_l = [\mathbf{0}_{N\times N}, \mathbf{I}_{N\times N}]$ in Eq. (24f). As the formulation Eq. (23) is homogeneous in terms of $\mathbf{w}$, we assume that the complex weights are included in the unit Euclidean ball. We define a slack variable $\mathbf{t}$ to relax the non-convex cardinality constraint in Eq. (24f) and transform the l_0 norm to the second-order cone programming (SOCP) as shown in Eq. (28e).

$$\begin{aligned}
\max_{\tilde{\mathbf{w}},\mathbf{t}} \quad & \mathbf{t}^T(\mathbf{t}-\mathbf{1}), && \text{(28a)}\\
\text{s.t.} \quad & \tilde{\mathbf{w}}^H\tilde{\mathbf{U}}_i\tilde{\mathbf{w}} \le 1+\delta, i=1,\ldots,p, && \text{(28b)}\\
& \tilde{\mathbf{w}}^H\tilde{\mathbf{U}}_i\tilde{\mathbf{w}} \ge 1-\delta, i=1,\ldots,p, && \text{(28c)}\\
& \tilde{\mathbf{V}}^H(\mathcal{J})\tilde{\mathbf{w}} = 0, && \text{(28d)}\\
& \text{or } \tilde{\mathbf{w}}^H\tilde{\mathbf{A}}_i\tilde{\mathbf{w}} \le \epsilon, i=1,\ldots,L,\\
& \tilde{\mathbf{w}}_i^2 + \tilde{\mathbf{w}}_{i+N}^2 \le t_i, i=1,\ldots,N, && \text{(28e)}\\
& 0 \le \mathbf{t} \le 1, && \text{(28f)}\\
& \mathbf{1}^T\mathbf{t} = K. && \text{(28g)}
\end{aligned}$$

Note that both the objective function in Eq. (28a) and the lower bound constraint imposed on the mainlobe in Eq. (28c) are non-convex. Similar to Eq. (15), we utilize the SCP as a local heuristic that leverages the ability to efficiently solve convex optimization problems. The $(k+1)$th iteration of the deterministic design based on the kth solution $\tilde{\mathbf{w}}^{(k)}$ and $\mathbf{t}^{(k)}$ can be written as,

$$\begin{aligned}
\max_{\tilde{\mathbf{w}},\mathbf{t}} \quad & (2\mathbf{t}^{(k)}-\mathbf{1})^T\mathbf{t} - \mathbf{t}^{(k)T}\mathbf{t}^{(k)}, && \text{(29)}\\
\text{s.t.} \quad & 2\tilde{\mathbf{w}}^{(k)H}\tilde{\mathbf{U}}_i\tilde{\mathbf{w}} - \tilde{\mathbf{w}}^{(k)H}\tilde{\mathbf{U}}_i\tilde{\mathbf{w}}^{(k)} \le 1+\delta, i=1,\ldots,p,\\
& 2\tilde{\mathbf{w}}^{(k)H}\tilde{\mathbf{U}}_i\tilde{\mathbf{w}} - \tilde{\mathbf{w}}^{(k)H}\tilde{\mathbf{U}}_i\tilde{\mathbf{w}}^{(k)} \ge 1-\delta, i=1,\ldots,p,\\
& \tilde{\mathbf{V}}^H(\mathcal{J})\tilde{\mathbf{w}} = 0,\\
& \text{or } \tilde{\mathbf{w}}^H\tilde{\mathbf{A}}_i\tilde{\mathbf{w}} \le \epsilon, i=1,\ldots,L,\\
& \tilde{\mathbf{w}}_i^2 + \tilde{\mathbf{w}}_{i+N}^2 \le t_i, i=1,\ldots,N\\
& 0 \le \mathbf{t} \le 1,\\
& \mathbf{1}^T\mathbf{t} = K.
\end{aligned}$$

Several runs with different feasible points should be carried out and the best K-antenna sparse array with the weight $\mathbf{w}$ is chosen as the final choice. A phase-only reconfigurable array can be achieved by restricting the modulus of weight coefficients to a constant and synthesizing the desired pattern by changing the phase only [31].

V. MSNR and Semi-Adaptive Beamformer Design with Controlled Quiescent Pattern

Although superior in maximizing the output SNR, both the MSNR and semi-adaptive beamformers ignore the shape of the quiescent pattern, such as sidelobe levels. Below, we combine the adaptive and deterministic approaches, in sections III and IV respectively, to offer a generalized metric for sparse array beamformer design. The associated optimization problem becomes more involved due to the additional sidelobe controlling constraints. We take the form of the sidelobe constraints in Eq. (24d) as an example in the following derivation.

A. Sparse Array MSNR Beamformer Design with Controlled Quiescent Pattern

Since it is not straightforward to adapt the iterative affine approximation to be compatible with the deterministic design, we utilize the frame based approximation to design the MSNR beamformer with controlled quiescent pattern. Thus, the formulation is similar to Eq. (22) with an additional sidelobe level constraint. That is,

$$\begin{aligned}
\max_{\mathbf{z}} \quad & \frac{\mathbf{e}_1^H\text{diag}(\mathbf{z})\mathbf{U}\mathbf{C}_s\mathbf{U}^H\text{diag}(\mathbf{z})\mathbf{e}_1}{\mathbf{e}_1^H\text{diag}(\mathbf{z})\mathbf{e}_1}, && \text{(30)}\\
\text{s.t.} \quad & \mathbf{e}_1^H\text{diag}(\mathbf{z})\mathbf{V}(\mathcal{J}) = \mathbf{0},\\
& \mathbf{z} \in \{0,1\}^N,\ \mathbf{1}^T\mathbf{z} = K.
\end{aligned}$$

Define the vector $\bar{\mathbf{e}}_1 = \mathbf{e}_1^* \odot \mathbf{e}_1$, the matrices $\bar{\mathbf{V}} = [\mathbf{e}_1^* \odot \mathbf{v}_1, \ldots, \mathbf{e}_1^* \odot \mathbf{v}_{|\mathcal{J}|}]$ and $\bar{\mathbf{U}} = [\mathbf{e}_1^* \odot \mathbf{u}_1, \ldots, \mathbf{e}_1^* \odot \mathbf{u}_p]$ with * denoting conjugate operation. The problem in Eq. (30) can be rewritten in the form of quadratic fractional,

$$\begin{aligned}
\max_{\mathbf{z}} \quad & \frac{\mathbf{z}^H\bar{\mathbf{U}}\mathbf{C}_s\bar{\mathbf{U}}^H\mathbf{z}}{\mathbf{z}^H\bar{\mathbf{e}}_1}, && \text{(31)}\\
\text{s.t.} \quad & \mathbf{z}^H\bar{\mathbf{V}} = 0,\\
& 0 \le \mathbf{z} \le 1,\ \mathbf{1}^T\mathbf{z} = K.
\end{aligned}$$

We relax the binary constraints $\mathbf{z} \in \{0,1\}^N$ to the box constraint $0 \le \mathbf{z} \le 1$, as the global maximizer of a quasi-convex function locates at the extreme points of the polyhedron [25], [32]. We propose an iterative linear fractional programming (ILFP) algorithm to solve the quadratic fractional. The problem in the $(k+1)$th iteration based on the kth solution $\mathbf{z}^{(k)}$ is written as,

$$\begin{aligned}
\max_{\mathbf{z}} \quad & \frac{2\mathbf{z}^{(k)H}\bar{\mathbf{U}}\mathbf{C}_s\bar{\mathbf{U}}^H\mathbf{z} - \mathbf{z}^{(k)H}\bar{\mathbf{U}}\mathbf{C}_s\bar{\mathbf{U}}^H\mathbf{z}^{(k)}}{\mathbf{z}^H\bar{\mathbf{e}}_1}, && \text{(32)}\\
\text{s.t.} \quad & \mathbf{z}^H\bar{\mathbf{V}} = 0,\\
& 0 \le \mathbf{z} \le 1,\ \mathbf{1}^T\mathbf{z} = K.
\end{aligned}$$

The linear fractional programming in Eq. (32) can be further transformed into a LP utilizing the Charnes-Cooper transformation [33] as follows,

$$\begin{aligned}
\max_{\mathbf{y},\alpha} \quad & 2\mathbf{z}^{(k)H}\bar{\mathbf{U}}\mathbf{C}_s\bar{\mathbf{U}}^H\mathbf{y} - \mathbf{z}^{(k)H}\bar{\mathbf{U}}\mathbf{C}_s\bar{\mathbf{U}}^H\mathbf{z}^{(k)}\alpha, && \text{(33)}\\
\text{s.t.} \quad & \mathbf{y}^H\bar{\mathbf{V}} = 0,\\
& \mathbf{1}^T\mathbf{y} = K\alpha,\ 0 \le \mathbf{y} \le \alpha,\\
& \alpha > 0,\ \bar{\mathbf{e}}_1^H\mathbf{y} = 1.
\end{aligned}$$

The optimum selection vector is finally obtained by $\mathbf{z} = \mathbf{y}/\alpha$. The highest computational complexity of the ILFP is of order kn^2m using an interior-point based method, with n, m and k denoting the respective numbers of variables, constraints and iterations [27]. Empirical results show that no more than ten iterations, that is $k \le 10$, are required for the ILFP algorithm to converge. Thus, the computational complexity of the ILFP is comparable to that of the LP, which can be accelerated by diverse solvers in the literature [34], [35].

B. Sparse Array Semi-Adaptive Beamformer Design Using ILFP

Let β in Eq. (8) be $\beta = \text{diag}(\gamma)\eta = [\gamma_1 e^{j\phi_1}, \ldots, \gamma_p e^{j\phi_p}]$ with $\gamma = [\gamma_1, \ldots, \gamma_p]$ denoting amplitude vector and $\eta = [e^{j\phi_i}, \ldots, e^{j\phi_p}]$ denoting phase vector. For approximately equal response beamforming, $\gamma_i = 1, i = 1, \ldots, p$. The desired beamformer can be expressed as,

$$\mathbf{w} = \mathbf{U}\text{diag}(\gamma)\eta = \sum_{i=1}^{p} \gamma_i e^{j\phi_i} \mathbf{u}_i. \tag{34}$$

Note that the coefficient amplitudes $\gamma_i, i = 1, \ldots, k$ are user-specified to approximate a desired pattern response. The coefficient phases, on the other hand, can be utilized as a free parameter for enhancing the semi-adaptive beamformer's performance. The optimum coefficient phase can be obtained by maximizing the output SNR in Eq. (10), i.e.,

$$\hat{\eta} = \text{argmax} \left\{ \frac{\eta^H \text{diag}(\gamma)\mathbf{U}^H \mathbf{R}_s \mathbf{U}\text{diag}(\gamma)\eta}{\eta^H \text{diag}(\gamma)\mathbf{U}^H \mathbf{U}\text{diag}(\gamma)\eta} \right\}. \tag{35}$$

Clearly, $\hat{\eta}$ is the principal eigenvector of the following matrix,

$$\hat{\eta} = \mathcal{P}\{(\mathbf{U}^H\mathbf{U})^{-1}(\mathbf{U}^H\mathbf{R}_s\mathbf{U})\} = \mathcal{P}\{\mathbf{C}_s\mathbf{U}^H\mathbf{U}\}. \tag{36}$$

Subsequently, element-wise normalization $\oslash$ is required,

$$\eta = \hat{\eta} \oslash |\hat{\eta}| = [\hat{\eta}_1/|\hat{\eta}_1|, \ldots, \hat{\eta}_p/|\hat{\eta}_p|]. \tag{37}$$

Note that the coefficient phase η is array-dependent. The optimum semi-adaptive beamformer should be configured in a way such that the output SNR in Eq. (10) is maximized, i.e.,

$$\begin{aligned} \max_{\mathbf{z},\eta} \quad & \frac{\eta^H \hat{\mathbf{U}}^H \text{diag}(\mathbf{z})\mathbf{R}_s\text{diag}(\mathbf{z})\hat{\mathbf{U}}\eta}{\eta^H \hat{\mathbf{U}}^H \text{diag}(\mathbf{z})\hat{\mathbf{U}}\eta}, \\ \text{s.t.} \quad & \mathbf{z} \in \{0,1\}^N,\ \mathbf{1}^T\mathbf{z} = K, \end{aligned} \tag{38}$$

where $\hat{\mathbf{U}} = \mathbf{U}\text{diag}(\gamma)$. The design of semi-adaptive beamformer with controlled sidelobe level is formulated as,

$$\begin{aligned} \max_{\mathbf{z},\eta} \quad & \frac{\eta^H \hat{\mathbf{U}}^H \text{diag}(\mathbf{z})\mathbf{R}_s\text{diag}(\mathbf{z})\hat{\mathbf{U}}\eta}{\eta^H \hat{\mathbf{U}}^H \text{diag}(\mathbf{z})\hat{\mathbf{U}}\eta}, \\ \text{s.t.} \quad & \mathbf{V}^H(\mathcal{J})\text{diag}(\mathbf{z})\hat{\mathbf{U}}\eta = \mathbf{0}; \\ & \mathbf{z} \in \{0,1\}^N,\ \mathbf{1}^T\mathbf{z} = K. \end{aligned} \tag{39}$$

Clearly, the sparse array design problem with respect to the two variables, $\mathbf{z}$ and η, is highly non-convex. We adopt an alternating optimization method, which iteratively shifts between $\mathbf{z}$ and η, to solve Eq. (39). First, assuming the fixed coefficient phase η and utilizing the following property of Khatri-Rao product $\circ$,

$$\mathbf{A}\text{diag}(\mathbf{x})\mathbf{b} = (\mathbf{b}^T \circ \mathbf{A})\mathbf{x}, \tag{40}$$

we obtain

$$\mathbf{U}^H\text{diag}(\mathbf{z})\hat{\mathbf{U}}\eta = [(\hat{\mathbf{U}}\eta)^T \circ \mathbf{U}^H]\mathbf{z}, \tag{41}$$

$$\eta^H\hat{\mathbf{U}}^H\text{diag}(\mathbf{z})\hat{\mathbf{U}}\eta = \mathbf{z}^T[(\hat{\mathbf{U}}\eta) \circ (\hat{\mathbf{U}}\eta)^*]. \tag{42}$$

and

$$\mathbf{V}^H(\mathcal{J})\text{diag}(\mathbf{z})\hat{\mathbf{U}}\eta = [(\hat{\mathbf{U}}\eta)^T \circ \mathbf{V}^H(\mathcal{J})]\mathbf{z}. \tag{43}$$

Define the vector $\tau = (\hat{\mathbf{U}}\eta) \circ (\hat{\mathbf{U}}\eta)^*$, the matrices $\underline{\mathbf{U}} = (\hat{\mathbf{U}}\eta)^T \circ \mathbf{U}^H$ and $\underline{\mathbf{V}} = (\hat{\mathbf{U}}\eta)^T \circ \mathbf{V}^H(\mathcal{J})$. The problem in Eq. (39) can be rewritten in the form of quadratic fractional,

$$\begin{aligned} \max_{\mathbf{z}} \quad & \frac{\mathbf{z}^T\underline{\mathbf{U}}^H\mathbf{C}_s\underline{\mathbf{U}}\mathbf{z}}{\mathbf{z}^T\tau} \\ \text{s.t.} \quad & \underline{\mathbf{V}}\mathbf{z} = \mathbf{0}, \\ & \mathbf{0} \le \mathbf{z} \le 1,\ \mathbf{1}^T\mathbf{z} = K. \end{aligned} \tag{44}$$

Similar to the problem in Eq. (31), the ILFP algorithm can then be utilized to obtain the optimal semi-adaptive beamformer with controlled sidelobe level. Given the selected sparse array, the optimum coefficient phase can be calculated from Eqs. (36) and (37). The semi-adaptive beamformer design procedure is summarized in Table I. Note that the construction of sparse array beamformers comprises two intertwined steps, optimum sparse array design through antenna selection as elucidated above, and weight calculations either by Eq. (4) or Eq. (34) depending on the implemented beamformers.

TABLE I
THE DESIGN PROCEDURE OF SEMI-ADAPTIVE BEAMFORMER

Step 1	Set iteration number $k = 0$; Generate set $\mathcal{J}_K \subset \{1, \ldots, N\}$, Set $\eta = \mathbf{1}$, $\mathbf{z}^{(0)} = \mathbf{0}$ and $\mathbf{z}^{(0)}(\mathcal{J}_K) = 1$.
Step 2	Employ ILFP to solve the selection problem in Eq. (44).
Step 3	Compute $\hat{\eta} = \mathcal{P}\{\mathbf{C}_s\mathbf{U}^H\text{diag}(\mathbf{z}^{(k)})\mathbf{U}\}$ and normalize $\eta = \hat{\eta} \oslash |\hat{\eta}|$.
Step 4	If $\|\mathbf{z}^{(k)} - \mathbf{z}^{(k-1)}\|_2 \ge \delta$, set $k = k + 1$ and go to Step 2; Otherwise, terminate.

VI. SIMULATIONS

In this section, simulation results are presented to validate the proposed sparse array quiescent beamformer design.

A. Example 1

Consider $K = 8$ available antennas and $N = 16$ uniformly spaced positions with an inter-element spacing of $d = \lambda/2$. Assume that three uncorrelated source signals are impinging on the array from directions $\theta_1 = 65°, \theta_2 = 75°, \theta_3 = 125°$ with the respective SNR being 6dB, 3dB and 0dB. Assuming that all the information of the sources is known to the receiver, thus the MSNR beamformer weights can be calculated as the principal eigenvector of the source correlation matrix as stated by Eq. (4). We enumerate all the 12870 different configurations based on the MSNR beamformer and the results are plotted in Fig. 1 in an ascending order. Moreover, a semi-adaptive beamformer $\mathbf{w} = \mathbf{U}\beta$ with $|\gamma_i| = 1, i = 1, \ldots, 3$ is implemented for each sparse array and the corresponding output SNRs are also depicted in Fig. 1 for comparison. Note that the array coefficient phases $\eta_i, i = 1, \ldots, 3$ are calculated according to Eq. (36) for each sparse array.

The following remarks are in order: (1) The optimum sparse array implementing the MSNR beamformer can attain 16.5dB output SNR, which is 1.45dB higher than the worst array configuration. This underscores the importance of array configurations in determining the output SNR in interference-free and quiescent scenarios. (2) The semi-adaptive beamformer performs worse than the MSNR beamformer in terms of

output SNR. The maximum output SNR of the semi-adaptive beamformer is 16.04dB, which is the best sparse array that can offer approximately equal gain towards each source. (3) Array configurations also affect the performance of the semi-adaptive beamformer significantly, where the SNR difference between the best and worst sparse arrays is 3.31dB. (4) The output SNR of semi-adaptive beamformers demonstrates an increasing trend with regard to array configurations sorted ascendingly according to that of the MSNR beamformer. The optimum sparse arrays for the two beamformers are shown in Fig. 2, with filled dots denoting selected positions for locating antennas and cross for discarded. The beampatterns of the MSNR and semi-adaptive beamformers based on the respective optimum sparse arrays are plotted in Fig. 3. Clearly, the MSNR beamformer ignores the far and weak source in order to maximize the output SNR. This disadvantage is overcome by the semi-adaptive beamformer with a 0.46dB performance degradation. Note that both sparse arrays exhibit high sidelobe levels especially in the angular region around the three sources.

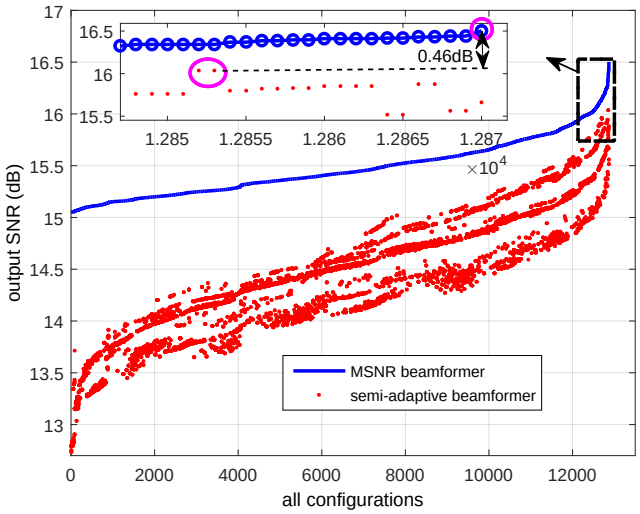

Fig. 1. Output SNRs of the MSNR and semi-adaptive beamfomers for all sparse arrays. The inner plot shows the output SNR difference.

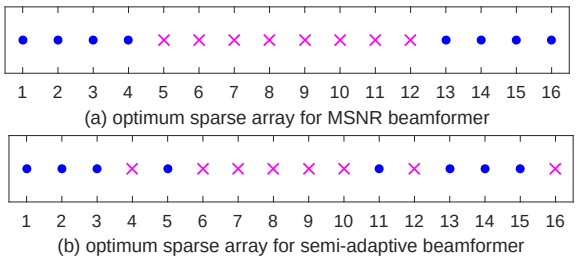

Fig. 2. Optimum sparse arrays for the MSNR and semi-adaptive beamformers.

B. Example 2

In this example, we verify the effectiveness of proposed antenna selection methods. There are two methods for constructing sparse MSNR beamformer, namely iterative affine approximation and frame based approximation solved by the

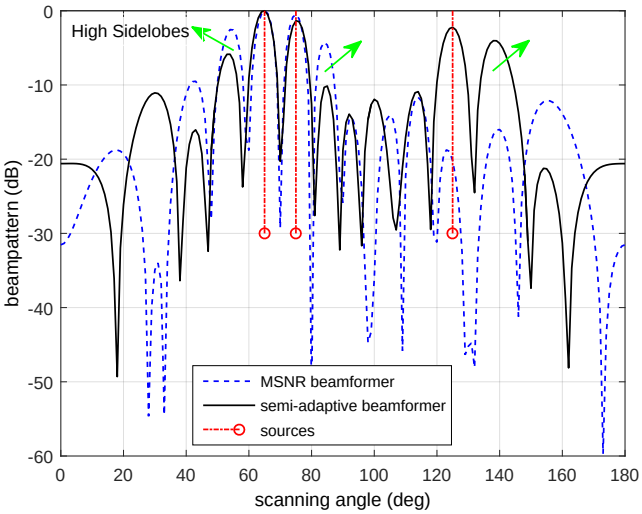

Fig. 3. Beampatterns of the MSNR and semi-adaptive beamfomers based on respective optimum sparse arrays. The green arrows indicate the unwanted high sidelobes.

ILFP algorithm. The ILFP algorithm is also used to reconfigure the semi-adaptive beamformer. We run 200 Monte-Carlo trials and three random integers uniformly generated within the range $[0, 180]$ are used for the sources' arriving angles in each trial. Optimum 8-antenna sparse arrays are selected based on the MSNR and semi-adaptive beamformers utilizing the two relaxation methods and the ILFP algorithm in each scenario. The output SNRs corresponding to the selected sparse arrays are calculated and those of true optimum arrays obtained through enumeration is used for the benchmark. The error distances between the two are plotted in the form of histogram in Fig. 4 (a), (b), (c). Furthermore, a summary of the simulation results is depicted in Fig. 4 (d), where the percentage of trials with the error distance smaller than a set of predefined threshold values is calculated. We can observe that the iterative affine approximation exhibits a slightly higher accuracy than the fame based approximation for the MSNR beamformer design, while 94.5% of the trials demonstrates less than 0.6dB error using both methods. For the semi-adaptive beamformer design, 90% of the trials achieve less than 0.4dB error using the ILFP algorithm. Nevertheless, the two relaxation methods and the ILFP algorithm perform equally well apart from a negligible and acceptable deviation from the true global optimum solutions. This again validates the effectiveness of proposed convex relation and iterative optimization methods.

C. Example 3

As already demonstrated in the Example 1, the beampatterns of selected optimum sparse arrays (a) and (b) exhibit high sidelobes for both beamformers since sidelobe constraints were not considered in the design procedure. We then calculate the optimum 8-antenna sparse MSNR and semi-adaptive beamformers with controlled sidelobes utilizing Eq. (33) and the method summarized in Table I. The sidelobes are required not to exceed -10dB with respect to the main peak. Smaller values of sidelobe levels reduce the output SNR and yield

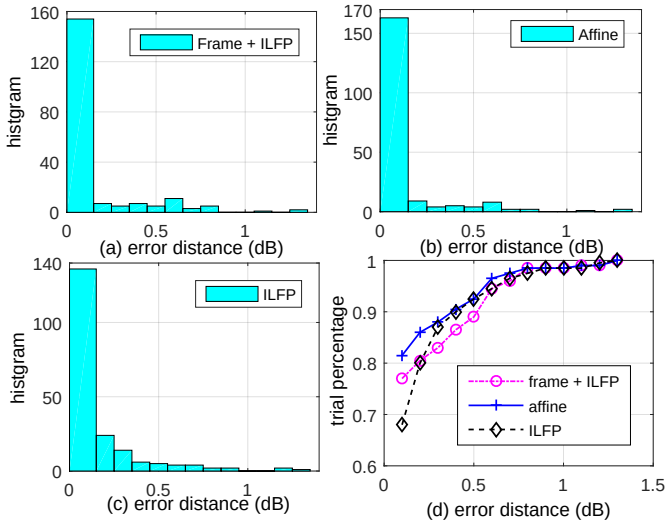

Fig. 4. (a) and (b) The error distance between output SNRs of true optimum arrays by enumeration and those of selected sparse array MSNR beamformer through frame based approximation and iterative affine approximation, respectively; (c) The error distance between output SNRs of true optimum arrays by enumeration and those of selected sparse array semi-adaptive beamformer through the ILFP algorithm; (d) The summary of simulation results in (a), (b), and (c).

highly distorted beampattern at unconstrained angles. The two selected optimum sparse arrays are shown in Fig. 5 (c) and (d). Their respective beampatterns are depicted in Fig. 6. Clearly, both arrays circumvent the high sidelobes in the angular region around the three sources. The weight calculation methods for both MSNR and semi-adaptive beamformers do not change, the sidelobe level are well maintained only through the proper choice of array reconfiguration. Once again, the array configuration is key to determine the beamforming performance.

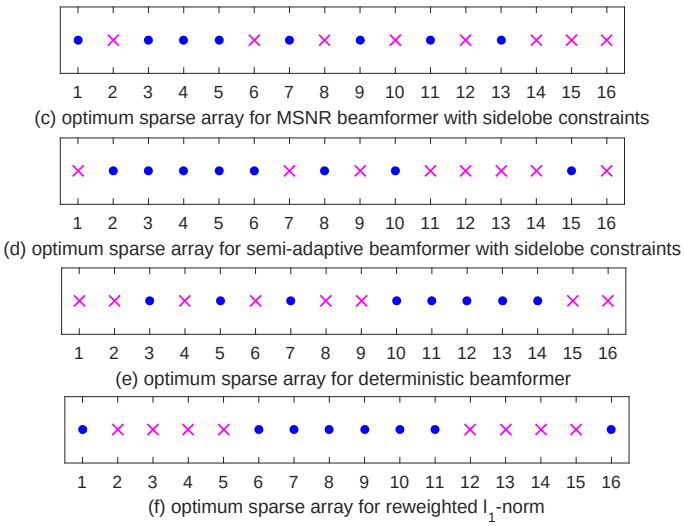

Fig. 5. Optimum sparse arrays for the MSNR, semi-adaptive, deterministic beamformers and reweighted l_1-norm method with sidelobe constraints.

In order to compare the (semi-)adaptive beamformer design with deterministic array synthesis, we implement the array thinning according to Eq. (29). The thinned array is shown in Fig. 5 (e) and the synthesized beampattern is plotted in

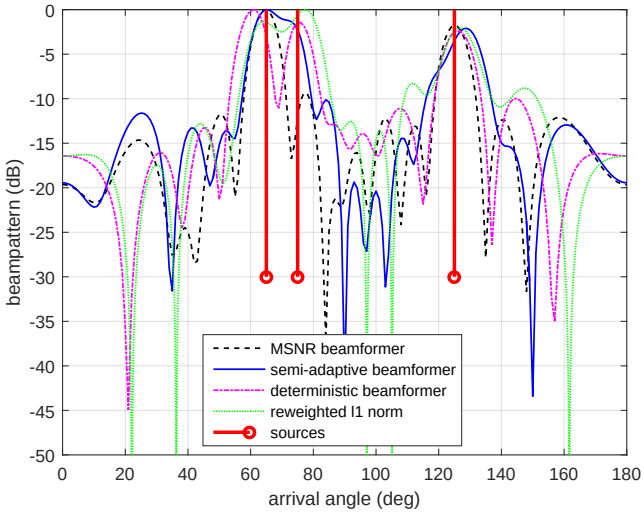

Fig. 6. Beampatterns of the MSNR, semi-adaptive, deterministic beamfomers and reweighted l_1-norm method based on respective optimum sparse arrays with sidelobe constraints.

pink dash-dot curve in Fig. 6, with the weights obtained from Eq. (29). For a comprehensive comparison, we also implement the deterministic sparse array synthesis based on the well-known reweighted l_1-norm method [17], [18], where the largest $K = 8$ coefficients are remained with others setting to zero. The corresponding sparse array is depicted in Fig. 5 (f) and its beampattern is plotted in green dot curve in Fig. 6. Clearly, all the three proposed beamformers successfully suppress the unwanted sidelobes by choosing respective suitable configurations. The deterministic beamformer exhibits a best-shaped response pattern, whereas the MSNR beamformer completely ignores the source arriving from 75° due to the additional sidelobe constraints. The semi-adaptive beamformer demonstrates a satisfactory compromise between the deterministic and the MSNR beamformers, although it fails to distinguish the first two closely-spaced sources. The sparse array configured through the reweighted l_1-norm method exhibits as high as -8.3dB sidelobes around the third source and broadened mainlobes around the first two closely-spaced sources.

D. Example 4

We examine the beamformer design in the case of correlated sources. Consider a distributed source arriving within the angular region $[75^\circ, 105^\circ]$. The source correlation is generated randomly with its absolute value bounded between zero and one. Suppose there are 12 antennas that can be placed in 20 uniformly-spaced positions. We implement antenna selection for the MSNR, semi-adaptive and deterministic beamformers with sidelobe constraints, and compare with the reweighted l_1-norm method. The four selected optimum sparse arrays are plotted in Fig. 7 (g), (h), (k) and (l). Their respective beampatterns are depicted in Fig. 8. We can observe the notable trade-off between mainlobe shape, such as mainlobe width and transition bandwidth, and sidelobe level. Again, the deterministic beamformer exhibits the best-shaped quiescent

pattern, and slightly better than that of the sparse array configured through the reweighted l_1-norm. The semi-adaptive beamformer demonstrates high sidelobe levels and the MSNR beamformer presents a poor mainlobe shape.

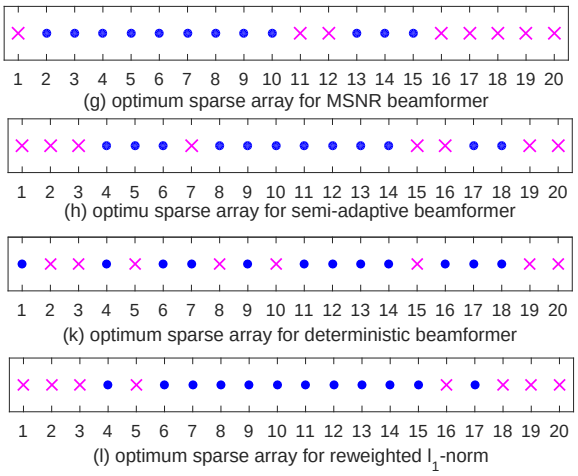

Fig. 7. Optimum sparse arrays for the MSNR, semi-adaptive, deterministic beamformers and reweighted l_1-norm with sidelobe constraints.

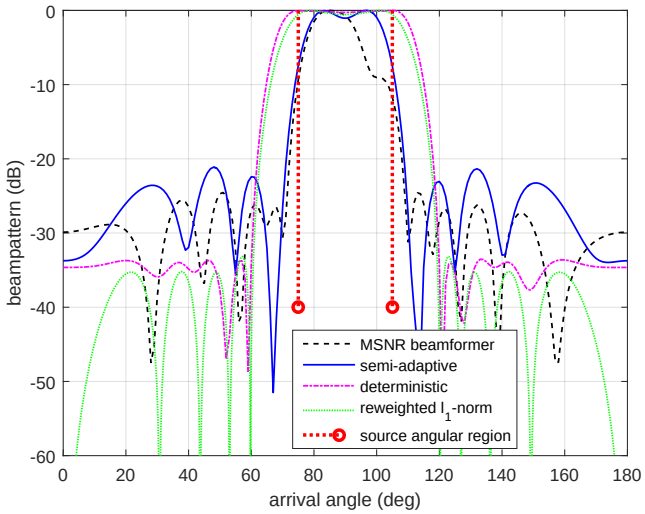

Fig. 8. Beampatterns of the MSNR, semi-adaptive, deterministic beamfomers and reweighted l_1-norm based on respective optimum sparse arrays with sidelobe constraints.

E. Example 5

For a further demonstration of the proposed sparse array quiescent beamformer design, we select 51 antennas out of 11×11 square array in terms of the MSNR beamformer with controlled sidelobe level. There are four discrete uncorrelated sources with 0dB SNR, arriving from $v_x = [-0.2, -0.3, 0.8, 0.65]$ and $v_y = [0.4, -0.6, 0.6, -0.4]$ in two-dimensional electronic angles, where $v_x = \cos\theta\cos\psi$ and $v_y = \cos\theta\sin\psi$ with θ and ψ denoting elevation and azimuth angles, respectively. The normalized beampattern of the selected 51-antenna optimum sparse array is plotted in Fig. 9. The sparse array is shown on the left of Fig. 10 and the contour of the beampattern is on the right. The output SNR of the sparse array MSNR beamformer is 20.72dB with -14dB peak sidelobe level (PSL) as indicated in the last row of the Table II.

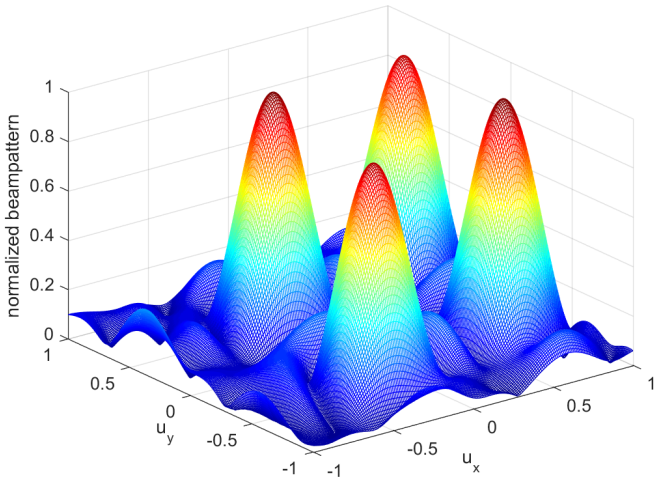

Fig. 9. Normalized beampattern of the MSNR beamfomer based on the selected 51-antenna sparse array with sidelobe constraints.

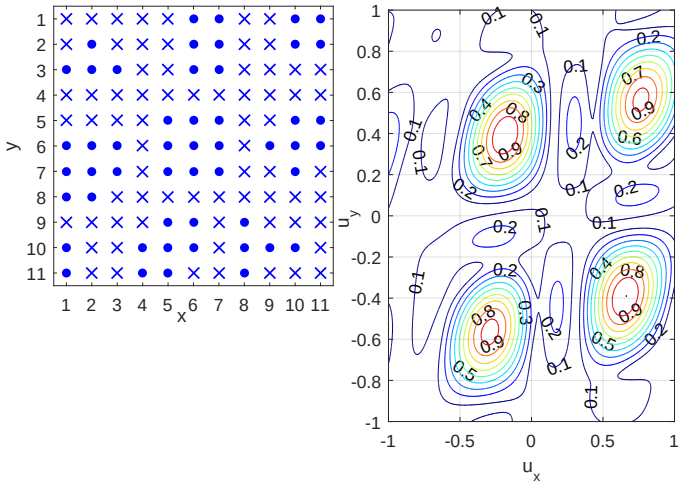

Fig. 10. The left: the selected 51-antenna sparse array (n); The right: the contour of the beampattern.

Finally, we compare the output SNR and PSL of the eleven selected sparse arrays (a)-(n) in table II. No doubt that the MSNR beamformer achieves the maximum output SNR, however it ignores some weak sources and exhibits poor quiescent pattern. The semi-adaptive beamformer overcomes the first disadvantage of the MSNR beamformer with an acceptable performance loss. The quiescent beampattern of both beamformers can be regularized by adding sidelobe constraints. The deterministic beamformer demonstrates the worst output SNR, whereas its advantage is manifested by the well-controlled sidelobes. The beamformer design combining both adaptive and deterministic constraints offers a compromise between the output SNR and quiescent beampatterns. The reweighted l_1-norm performs worse especially when dealing with unsymmetric beampattern as it assumes symmetric array configuration and conjugate weight coefficients. The optimum

TABLE II
THE OUTPUT SNR, PSL AND COMPUTATIONAL TIME OF EACH ARRAY.

Array Name	SNR (dB)	PSL (dB)	beamformer	sidelobe constraints	time sec
(a)	16.5	-2.54	MSNR	No	0.52
(b)	16.04	-4.05	semi-adaptive	No	0.65
(c)	16.17	-9.89	MSNR	Yes	1.19
(d)	14.84	-10.12	semi-adaptive	Yes	1.20
(e)	13.55	-10	deterministic	Yes	1.80
(f)	13.66	-8.3	reweighted l_1	Yes	1.67
(g)	15.56	-24.72	MSNR	Yes	1.86
(h)	15.31	-21.34	semi-adaptive	Yes	1.95
(k)	10.91	-33.54	deterministic	Yes	2.37
(l)	11.18	-33.18	reweighted l_1	Yes	1.6
(n)	20.72	-14	MSNR	Yes	3.13

sparse array is calculated by the CVX software [36] embedded in MATLAB using a desktop with 3.4GHz Intel i7-CPU and 16GB RAM. The computational times are listed in the last column of Table II and demonstrate comparable values to the benchmark of the well-known reweighted l_1-norm algorithm.

VII. CONCLUSION

We examined the problem of optimum sparse array beamformer design through antenna selection in the presence of multiple desired sources in interference-free environment. Two beamformers, namely the MSNR and semi-adaptive beamformers, were considered and compared with the deterministic design. Unlike other work in the literature, we utilized the array configuration as an additional DoF to improve the beamforming performance without concerning with complicated beamformer design. We proposed a general sparse array design metric combining adaptive and deterministic approaches, where the reconfigured beamformers exhibited well-controlled sidelobes with an acceptable performance loss. Simulation results validated the important role of array configurations in determining the beamforming performance in interference-free environments. The sparse array quiescent beamformer designed by proposed metrics demonstrated a welcome compromise between output SNR and desired response pattern.

REFERENCES

[1] B. Widrow, P. E. Mantey, L. J. Griffiths, and B. B. Goode, "Adaptive antenna systems," *Proceedings of the IEEE*, vol. 55, pp. 2143–2159, Dec 1967.

[2] S. Applebaum, "Adaptive arrays," *Antennas and Propagation, IEEE Transactions on*, vol. 24, no. 5, pp. 585–598, 1976.

[3] K. Buckley and L. Griffiths, "An adaptive generalized sidelobe canceller with derivative constraints," *IEEE Transactions on Antennas and Propagation*, vol. 34, pp. 311–319, Mar 1986.

[4] B. D. V. Veen and K. M. Buckley, "Beamforming: a versatile approach to spatial filtering," *IEEE ASSP Magazine*, vol. 5, pp. 4–24, April 1988.

[5] H. Lin, "Spatial correlations in adaptive arrays," *Antennas and Propagation, IEEE Transactions on*, vol. 30, no. 2, pp. 212–223, 1982.

[6] X. Wang, E. Aboutanios, M. Trinkle, and M. Amin, "Reconfigurable adaptive array beamforming by antenna selection," *Signal Processing, IEEE Transactions on*, vol. 62, pp. 2385–2396, May 2014.

[7] X. Wang, E. Aboutanios, and M. G. Amin, "Slow radar target detection in heterogeneous clutter using thinned space-time adaptive processing," *IET Radar, Sonar Navigation*, vol. 10, no. 4, pp. 726–734, 2016.

[8] Ö. T. Demir and T. E. Tuncer, "Optimum discrete phase-only transmit beamforming with antenna selection," in *Signal Processing Conference (EUSIPCO), 2014 Proceedings of the 22nd European*, pp. 1282–1286, IEEE, 2014.

[9] Ö. T. Demir and T. E. Tuncer, "Optimum discrete transmit beamformer design," *Digital Signal Processing*, vol. 36, pp. 57–68, 2015.

[10] H. L. Van Trees, *Detection, estimation, and modulation theory, optimum array processing*. John Wiley & Sons, 2004.

[11] O. Bucci, G. D'Elia, G. Mazzarella, and G. Panariello, "Antenna pattern synthesis: A new general approach," *Proceedings of the IEEE*, vol. 82, no. 3, pp. 358–371, 1994.

[12] C. Tseng and L. Griffiths, "A simple algorithm to achieve desired patterns for arbitrary arrays," *Signal Processing, IEEE Transactions on*, vol. 40, no. 11, pp. 2737–2746, 1992.

[13] R. Compton Jr, "The relationship between tapped delay-line and FFT processing in adaptive arrays," *Antennas and Propagation, IEEE Transactions on*, vol. 36, no. 1, pp. 15–26, 1988.

[14] L. J. Griffiths and K. Buckley, "Quiescent pattern control in linearly constrained adaptive arrays," *Acoustics, Speech and Signal Processing, IEEE Transactions on*, vol. 35, no. 7, pp. 917–926, 1987.

[15] B. D. V. Veen, "Optimization of quiescent response in partially adaptive beamformers," *IEEE Transactions on Acoustics, Speech, and Signal Processing*, vol. 38, pp. 471–477, Mar 1990.

[16] X. Wang, M. G. Amin, and X. Cao, "Optimum array configurations of maximum output SNR for quiescent beamforming," in *2017 IEEE International Conference on Acoustics, Speech and Signal Processing (ICASSP)*, pp. 6274–6278, March 2017.

[17] S. Nai, W. Ser, Z. Yu, and H. Chen, "Beampattern synthesis for linear and planar arrays with antenna selection by convex optimization," *Antennas and Propagation, IEEE Transactions on*, vol. 58, no. 12, pp. 3923–3930, 2010.

[18] B. Fuchs, "Application of convex relaxation to array synthesis problems," *Antennas and Propagation, IEEE Transactions on*, vol. 62, pp. 634–640, Feb 2014.

[19] Y. Liu, L. Zhang, L. Ye, Z. Nie, and Q. H. Liu, "Synthesis of sparse arrays with frequency-invariant-focused beam patterns under accurate sidelobe control by iterative second-order cone programming," *IEEE Transactions on Antennas and Propagation*, vol. 63, no. 12, pp. 5826–5832, 2015.

[20] B. Fuchs and S. Rondineau, "Array pattern synthesis with excitation control via norm minimization," *IEEE Transactions on Antennas and Propagation*, vol. 64, no. 10, pp. 4228–4234, 2016.

[21] S. Joshi and S. Boyd, "Sensor selection via convex optimization," *Signal Processing, IEEE Transactions on*, vol. 57, no. 2, pp. 451–462, 2009.

[22] E. Candes, M. Wakin, and S. Boyd, "Enhancing sparsity by reweighted l1 minimization," *Journal of Fourier Analysis and Applications*, vol. 14, no. 5, pp. 877–905, 2008.

[23] X. Wang, E. Aboutanios, and M. Amin, "Thinned array beampattern synthesis by iterative soft-thresholding-based optimization algorithms," *Antennas and Propagation, IEEE Transactions on*, vol. 62, pp. 6102–6113, Dec 2014.

[24] G. Oliveri, M. Carlin, and A. Massa, "Complex-weight sparse linear array synthesis by bayesian compressive sampling," *Antennas and Propagation, IEEE Transactions on*, vol. 60, no. 5, pp. 2309–2326, 2012.

[25] H. Tuy, *Convex analysis and global optimization*. Springer, 1998.

[26] R. A. Horn and C. R. Johnson, *Matrix analysis*. Cambridge university press, 2012.

[27] S. Boyd and L. Vandenberghe, *Convex optimization*. Cambridge university press, 2004.

[28] J. Kovacevic and A. Chebira, "Life beyond bases: The advent of frames," *IEEE Signal Processing Magazine*, 2007.

[29] N. I. Akhiezer and I. M. Glazman, *Theory of linear operators in Hilbert space*. Courier Corporation, 2013.

[30] D. Han and D. R. Larson, *Frames, bases and group representations*, vol. 697. American Mathematical Soc., 2000.

[31] T. Isernia, A. Massa, A. F. Morabito, and P. Rocca, "On the optimal synthesis of phase-only reconfigurable antenna arrays," in *Proceedings of the 5th European Conference on Antennas and Propagation (EUCAP)*, pp. 2074–2077, April 2011.

[32] R. Horst, *Introduction to global optimization*. Springer, 2000.

[33] A. Charnes and W. W. Cooper, "Programming with linear fractional functionals," *Naval Research logistics quarterly*, vol. 9, no. 3-4, pp. 181–186, 1962.

[34] H. Crowder, E. L. Johnson, and M. Padberg, "Solving large-scale zero-one linear programming problems," *Operations Research*, vol. 31, no. 5, pp. 803–834, 1983.

[35] J. Mattingley and S. Boyd, "Real-time convex optimization in signal processing," *IEEE Signal processing magazine*, vol. 27, no. 3, pp. 50–61, 2010.

[36] M. Grant, S. Boyd, and Y. Ye, "CVX: Matlab software for disciplined convex programming," 2008.

Xiangrong Wang received the the B.Eng and M.Eng degrees in electrical engineering from Nanjing University of Science and Technology, China, in 2009 and 2011, respectively, and the Ph.D. degree in signal processing in University of New South Wales, Australia in 2015. She was a post-doctoral research fellow in the Center for Advanced Communications, Villanova University, USA from Feb to Sep in 2016. Currently, she is an associate professor in the School of Electronic and Information Engineering, Beihang University, China. Her research interest includes adaptive array processing, DOA estimation, convex optimization and intelligent signal processing.

Moeness Amin received the B.Sc. degree from the Faculty of Engineering, Cairo University in 1976, M,Sc from University of Petroleum and Minerals in 1980, and a Ph.D. degree in electrical engineering from the University of Colorado, Boulder, in 1984. Since 1985, he has been with the Faculty of the Department of Electrical and Computer Engineering, Villanova University, Villanova, PA, USA, where he became the Director of the Center for Advanced Communications, College of Engineering, in 2002. Dr. Amin is a Fellow of the Institute of Electrical and Electronics Engineers; Fellow of the International Society of Optical Engineering; Fellow of the Institute of Engineering and Technology; and a Fellow of the European Association for Signal Processing. He is the Recipient of the 2017 Fulbright Distinguished Chair in Advanced Science and Technology; Recipient of the 2016 Alexander von Humboldt Research Award; Recipient of the 2016 IET Achievement Medal; Recipient of the 2014 IEEE Signal Processing Society Technical Achievement Award; Recipient of the 2010 NATO Scientific Achievement Award; Recipient of the 2009 Individual Technical Achievement Award from the European Association for Signal Processing; Recipient of the 2015 IEEE Aerospace and Electronic Systems Society Warren D White Award for Excellence in Radar Engineering; and Recipient of the 2010 Chief of Naval Research Challenge Award. Dr. Amin is the Recipient of the IEEE Third Millennium Medal. He was a Distinguished Lecturer of the IEEE Signal Processing Society, 2003-2004, and is the past Chair of the Electrical Cluster of the Franklin Institute Committee on Science and the Arts. Dr. Amin has over 750 journal and conference publications in signal processing theory and applications, covering the areas of Wireless Communications, Radar, Sonar, Satellite Navigations, Ultrasound, Healthcare, and RFID. He has co-authored 21 book chapters and is the Editor of three books titled, Through the Wall Radar Imaging, Compressive Sensing for Urban Radar, Radar for Indoor Monitoring, published by CRC Press in 2011, 2014, 2017, respectively.

Xianghua Wang received the B.Eng degree in Automation from Northwestern Polytechnical University, Xian, China, in 2010 and the Ph.D. degree in Mechanical System and Control from Peking University, Beijing, China, in 2015. She is currently a senior lecturer at the Shandong University of Science and Technology. Her current research interests include fault estimation, optimization, and guidance and control of aerospace systems.

Xianbin Cao received the B.Eng and M.Eng degrees in computer applications and information science from Anhui University, China, in 1990 and 1993, respectively, and the Ph.D. degree in information science from the University of Science and Technology of China, in 1996. He is currently the Dean and Professor of the School of Electronic and Information Engineering, Beihang University, Beijing, China. His current research interests include intelligent transportation systems, airspace transportation management, and intelligent computation.